PHILOSOPHICAL TRANSACTIONS OF THE ROYAL SOCIETY A
MATHEMATICAL, PHYSICAL & ENGINEERING SCIENCES

Toward a composite orbital chronology for the Late Cretaceous and Early Palaeocene GPTS

Timothy D. Herbert

Phil. Trans. R. Soc. Lond. A 1999 **357**, 1891-1905
doi: 10.1098/rsta.1999.0406

THE ROYAL SOCIETY

Toward a composite orbital chronology for the Late Cretaceous and Early Palaeocene GPTS

By Timothy D. Herbert

Department of Geological Sciences, Brown University, Providence, RI 02912, USA

Drill sites recovered from the South Atlantic by the Deep Sea Drilling Project provide excellent magnetostratigraphies for the time-interval of polarity chrons C33r through C28n (83–62.5 Ma: Cande & Kent time-scale). Cyclic patterns of carbonate sedimentation, with a mean repeat time of *ca.* 20 ka, can be correlated between sites. The cycles show the full hierarchy of eccentricity amplitude modulations that would be expected of precessional orbital forcing. A significant modulation component exists at *ca.* 400 ka, which in all likelihood matches the modern 404 ka repeat time for eccentricity. This modulation pattern may provide the 'tuning fork' for tying cyclical sedimentation to the most stable astronomical eccentricity period. A *ca.* 2.5 Ma modulation also emerges that seems surprisingly similar to the modern long-wavelength eccentricity modulation of precessional amplitude, which should average 2.425 Ma. Results of 'cyclochronology' of polarity chrons C29n–C31n suggest that the Cande & Kent time-scale will need to be revised to allow for a more gentle change in South Atlantic sea-floor spreading than modelled by those authors.

Keywords: carbonate cycles; Cretaceous; Palaeocene; magnetostratigraphy; eccentricity cycles; precessional cycles

1. Introduction

Both opportunities and dangers exist in developing orbitally tuned time-scales in strata older than the limit of precise astronomical solutions for the Earth's orbital variations. These older records may provide significant insights into the stability of the Earth's orbital elements, and document periods of transition predicted by chaotic solutions to the evolution of the Solar System (Laskar 1990, and this issue). Orbital tuning also may provide a quantum jump in the precision and accuracy of time-scales. For example, applying an optimistic relative error in radiometric dating of 0.5% yields numerical uncertainties of 325 000 years (325 ka) at the Cretaceous–Tertiary (K–T) boundary and significantly greater as one proceeds into the earlier Mesozoic. Added to this loss in numerical resolution is the decrease in number, and then disappearance due to subduction, of sea-floor reference sections for the geomagnetic polarity time-scale (GPTS). Dangers arise from a number of sources in applying orbital tuning methods to older sections. Independent age constraints on cycle durations, and our ability to correlate precisely between cyclical sequences, degrade over time. Furthermore, we are faced with the difficulty of constructing a continuous chronology in the absence of a firm orbital template (see Laskar, this issue).

The sedimentary records of Late Cretaceous and Early Palaeocene age discussed in this paper represent a reasonable trade-off between these prospects. Many sites are potentially available through ocean drilling; in addition many marine sections are exposed on land (cf. Ten Kate & Sprenger 1993). Magnetic reversal occurred frequently enough during the study time to provide useful tests of the orbital method, and to yield tie-points for constructing an integrated time-scale. The sea-floor record, although significantly reduced relative to that of the Neogene, still offers a good template for testing the implications of an orbitally derived time-scale for tectonic processes, as was used by Wilson (1993) to evaluate Shackleton *et al*.'s (1990) revision to the then-accepted Plio-Pleistocene GPTS. Radiometric dating, correlated to the GPTS, provides good constraints on the mean periods of sedimentary cycles, provided that one is willing to average records over several Ma windows. One more observation helps to fill in this optimistic picture. A number of studies suggest that the dominant pattern of Late Cretaceous and Early Palaeocene climate cyclicity follows a precessional driving force (Herbert & D'Hondt 1990; Park *et al*. 1993; Ten Kate & Sprenger 1993). Precession is a very nice signal for stratigraphic purposes, since it displays a hierarchy of modulating terms that should provide stratigraphically correlatable features. Of these terms, I draw special attention to the 404 ka eccentricity modulation, as this period is believed to be an unusually stable feature of the Earth's orbital solutions.

2. Stratigraphy of study sites

Assembling a Late Cretaceous–Early Palaeocene orbitally tuned GPTS requires patching records between sites, and testing an orbital chronometry where one can document stratigraphic overlap. The best guides at present come from palaeomagnetic reversal stratigraphy, and from the tie-line provided by the K–T extinction level, which also offers a link to a number of Ar/Ar radiometric age determinations (Cande & Kent 1995). Figure 1 displays some of the lithological data I obtained from a number of South Atlantic study sites (original data archived with the National Geophysical Data Centre, Boulder, CO), together with magnetostratigraphy (Hamilton & Suzyumov 1983; Chave 1984; Gee & Herbert 1999). Note that quite good coverage exists over the interval of chrons C31N through C28N. Cycle chronology for the interval of chrons C31R through C33R comes almost entirely from Deep Sea Drilling Project (DSDP) Site 516F, as the Walvis Ridge sites (Sites 525–529) bottomed in basaltic basement of ages ranging from 70 to 73 Ma (Moore *et al*. 1984). Site 357 was drilled not far from the location of Site 516F, but was discontinuously cored. I will demonstrate later that cyclic sections correlate very precisely between Site 357 and 516F; redrilling the Rio Grande Rise would almost certainly complete our chronology in the intervals of core gaps at Site 516F. Note also that while the precessional cycles characteristic of Late Cretaceous sedimentation persist at least through chron C25N at Site 516F, poor recovery in the Palaeocene section of most core sites prevents assembly of composite time-scale younger than chron C28N.

In the absence of true composite sections obtained by drilling multiple holes at the same location (cf. Ruddiman *et al*. 1987), our chronology must cope with the uncertainties caused by sections of core not recovered by drilling, which can range up to several metres. At compacted sedimentation rates typical of the South Atlantic sites (1–2 cm ka^{-1} in the Cretaceous, 0.5–1 cm ka^{-1} in the Palaeocene), coring omissions can therefore range up to 300 ka in the worst cases. Cores brought on board ship often contain less sediment than the nominally drilled 9.5 m. DSDP and Ocean

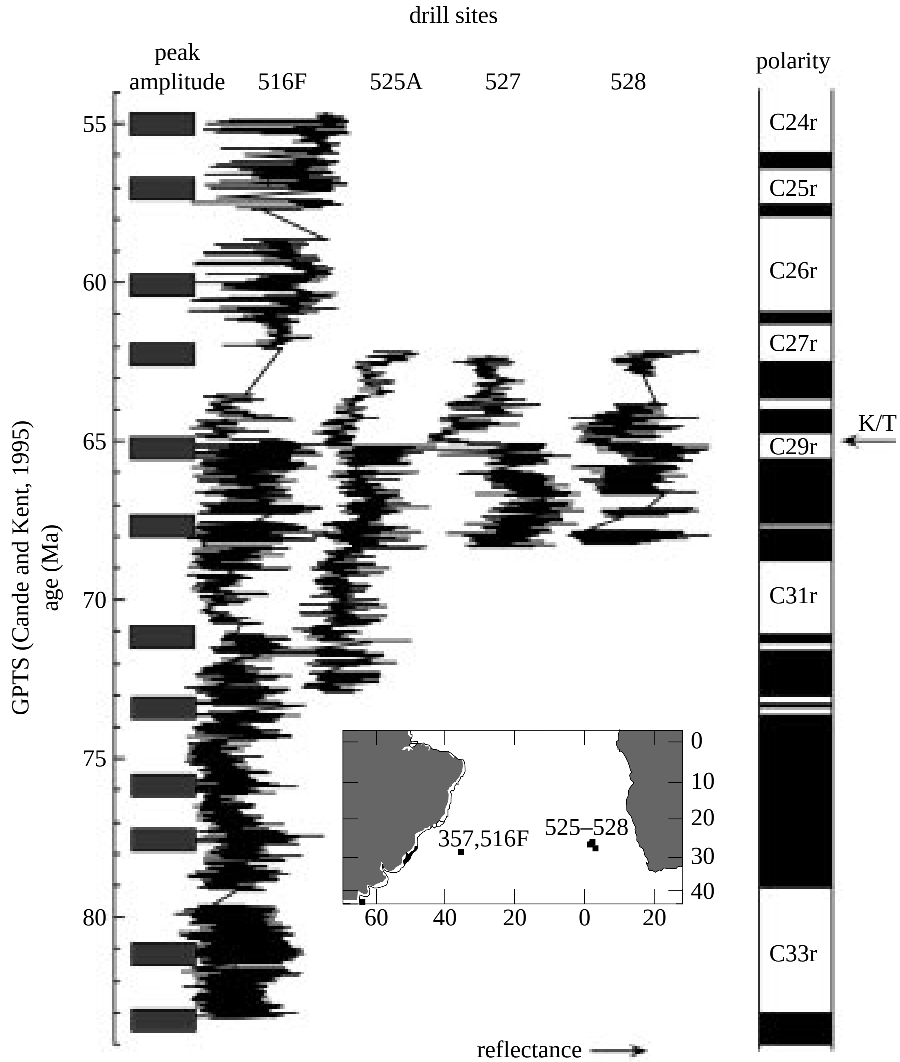

Figure 1. Reflectance (at 700 nm) data aquired on relatively continuously recovered Late Cretaceous–Palaeocene sequences from the South Atlantic. Reflectance provides an indirect measure of calcium carbonate content. The time-scale comes from magnetic polarity stratigraphy keyed to the GPTS of Cande & Kent (1995) ('GPTS' to the right of the sediment data). Large-scale organization of packets of high carbonate variance at *ca.* 2.5 Ma intervals is indicated by shaded boxes to the left of sediment data.

Drilling Program (ODP) convention place the top of recovered material at the top of the interval drilled, on the assumption that sediment tends to get lost from the base of the core as it comes up the hole to the drill ship. No documentation exists yet of whether rotary coring and core recovery actually work this way. I will follow this convention in the absence of positive indications of the placement of core gaps, but allow for repositioning data with gaps where data from other drill holes can be spliced convincingly into a composite sequence.

PHILOSOPHICAL TRANSACTIONS OF THE ROYAL SOCIETY A MATHEMATICAL, PHYSICAL & ENGINEERING SCIENCES

In addition to using the magnetostratigraphic data sources listed above, I have also used, wherever possible, foraminiferal (Premoli Silva & Boersma 1977; Boersma 1984) and nannofossil biostratigraphies (Perch-Nielsen 1977; Manivit & Feinberg 1984; Henriksson 1993) conducted at the study sites to confirm palaeomagnetic correlations of core intervals to the GPTS. The following briefly describes the stratigraphic control, range, and uncertainties of each study site discussed in this paper.

Site 357, Rio Grande Rise. Site 357 was discontinuously cored, with the result that 10 m coring gaps occur between recovered intervals. No palaeomagnetic studies were published as part of the original scientific investigation. Initial palaeomagnetic sampling (Gee & Herbert 1999) documents a normal below a reversed-polarity zone in core 30 (at *ca.* 479.2 m below sea floor (mbsf)) that approximately coincides with the nannofossil first-appearance datum event *E. macellus* (Perch-Nielsen 1977). The biostratigraphic constraint indicates that core 30 recovered parts of chrons C27r and C28n (Early Palaeocene). Core 31 contains dominantly normal polarities and a Late Maastrichtian fauna and flora. I assign this core to chron C30N. Core 32 contains a short reversed-polarity interval that corresponds to chron C30r (nominal duration of 125 ka (Cande & Kent 1995 GPTS)). Core 33 is entirely reversely magnetized and correlates to chron C31R. Core 34 contains a short reversed-polarity zone above a longer normally magnetized interval that places the sequence at the C31r–C32n boundary. Core 35 contains a brief normal polarity interval between reversely magnetized sections. I associate this normal polarity interval with chron C32r.1n. Core 36 is entirely of normal polarity, and belongs to polarity chron C33n. Recovery of cores 37 through 39 at Site 357 was poor; I have not included data from cores 40–49 (Lower Campanian–Santonian) in this study.

Site 516F, Rio Grande Rise. Site 516F was continuously cored, with better than 80% recovery from the latest Santonian–Early Palaeocene interval. We have supplemented shipboard magnetic studies with 262 new samples (Gee & Herbert 1999). These define chron C25n to lie between 907 and 913 mbsf and chron C25r to lie between 913 and 921.1 mbsf. A core recovery gap contains the chron C26n/C26r transition, chron C27n lies between 946.75 and 948.25 mbsf. Below a core recovery gap a reversed-polarity interval between 958.1 and 959.44 mbsf defines chron C28r. The K–T boundary occurs within chron C29r (base of chron at 971 mbsf, top at 962.8 mbsf) at 963.8 mbsf. Chron C30r is well defined in core 93 between 996.55 and 997.7 mbsf. The normal to reverse polarity transition at 1010.95 mbsf defines the C31n/C31r boundary. The base of polarity chron C31r is probably lost by poor core recovery in cores 95 and 96. A short reversed-polarity interval overlying a long normal polarity interval in core 97 (1029.86 mbsf) is interpreted to contain the C32n.1r to C32n.2n transition. Chron C32r occurs between 1059.6 and 1069.74 mbsf, although the short polarity chron C32r.1n is missing in a core recovery gap. The boundary between chrons C33n and C33r occurs at 1126.85 mbsf; the top of the long normal polarity interval occurs at 1197 mbsf.

Site 525A, Walvis Ridge. Site 525 contains a good record from the lower part of polarity chron C27r (Early Palaeocene) through mid C32n (Upper Campanian). We have supplemented Chave's (1984) excellent original magnetostratigraphy with

15 new samples to better define several polarity transitions. I interpret the short reversed-polarity interval in core 39 between 446.9 and 447.68 mbsf to correspond to chron C28r. Hole 525A bottomed in sediment of normal polarity corresponding to chron C32n.2n; ages of strata below the chron C32n.1r–C32n.2n boundary come from extrapolation of palaeomagnetically determined sedimentation rates above.

Site 527, Walvis Ridge. Site 527 contains a record of sedimentation that ranges from early chron C27r through late chron C31n (Early Palaeocene through Mid-Maastrichtian). Sediments contain frequent turbidites that interrupt pelagic chalk-marl oscillations. I follow the original magnetostratigraphy of Chave (1984), which defines most polarity boundaries to 20 cm or better resolution. The relatively short record length and less than optimal sedimentary character of Site 527 make it much less useful for cyclostratigraphic purposes than many of the other sites discussed.

Site 528, Walvis Ridge. Site 528 contains a similar record to that of Site 527, with the distinction that it recovered the interval containing chron C29r and the K–T boundary much better. Short chron C31r is lost in a core recovery gap between cores 35 and 36. Because of the abundant volcanogenic turbidites in the section below core 36, I did not attempt to extend my analysis before chron C31n at Site 528.

Site 529, Walvis Ridge. This hole contains the most expanded Danian (earliest Palaeocene) section of all the South Atlantic drill sites analysed (Herbert & D'Hondt 1990; D'Hondt *et al*. 1996). Unfortunately, the boundary between chrons C28r and C29n lies in a section of unrecovered sediment, and part of the Cretaceous interval of chron C29r contains contorted bedding indicating slumping. The hole terminates in a section of uncertain Late Cretaceous (older than chron C29r) age.

Most of the figures to follow will display lithological variations converted from stratigraphic depth to time using the Cande & Kent (1995) GPTS, which was also adopted by Berggren *et al*. (1995). The time-scales derived at each study site will therefore suffer from any errors in this GPTS, as well as from errors introduced by the assumption of constant sedimentation rates between palaeomagnetic tie-points. The cyclical variations documented below will therefore initially be presented independent of orbital 'tuning' methods. The reader should bear in mind the various sources of stratigraphic uncertainty, as well as the considerable consistency of results between study sites and the qualitative similarities between precessional forcing and lithological variations in the Late Cretaceous and Early Palaeocene of the South Atlantic, in assessing the orbital hypothesis.

3. Methods

Long time-series sampled at a mean sample spacing of 3 ka come from digital reflectance data acquired with a portable spectrometer (Minolta CM-2000) on the split surfaces of the DSDP cores. The instrument has been used successfully to log lithologic variations since Leg 154 of the Ocean Drilling Program (Curry *et al*. 1995). I determined the match of reflectance values to calcium carbonate content measured in discrete samples from the DSDP sites. Reflectance follows an exponential dependence on carbonate content. Regression estimates that express the relationship as

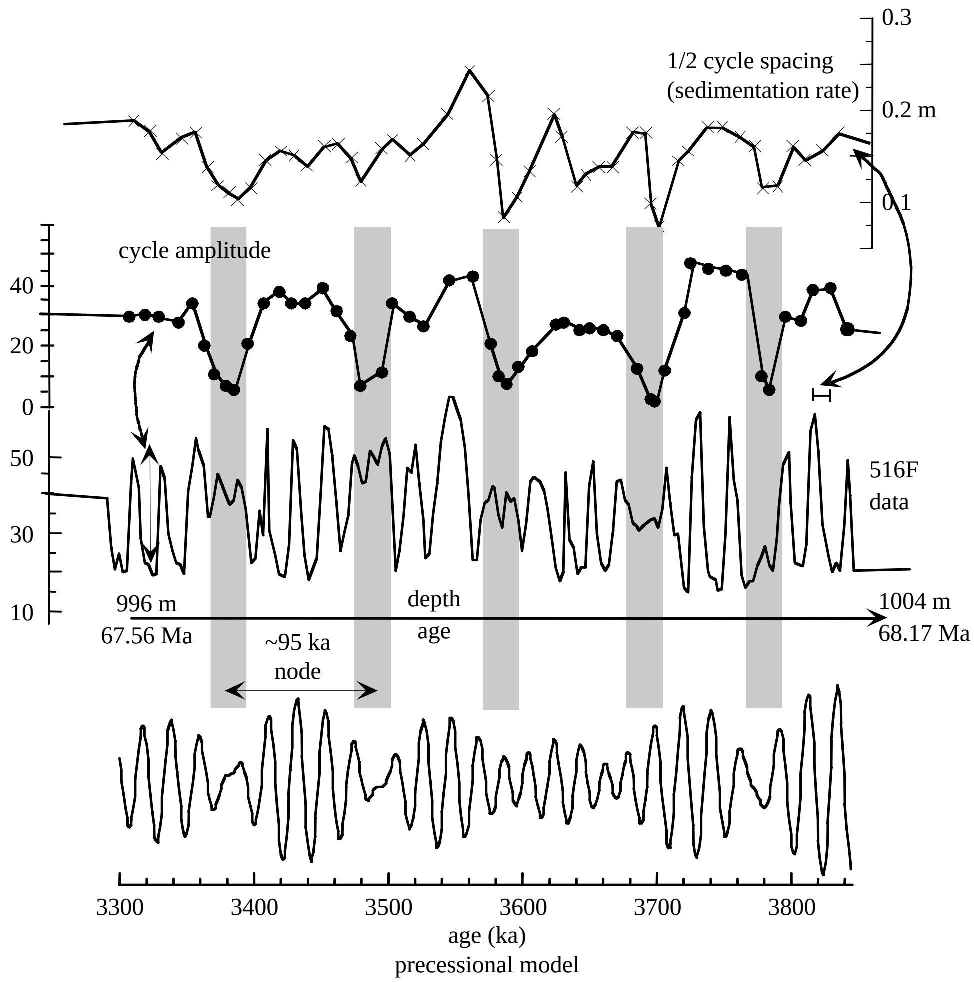

Figure 2. A detail of reflectance data taken from DSDP Site 516F. Note the cyclic repetition of two to three cycles of large reflectance contrast, followed by two to three cycles of lower-amplitude variations. The lower curve is a model precessional time-series (3.3–3.85 Ma) from Laskar *et al*. (1993) for comparison purposes. The upper two curves show how amplitude and thickness time-series are calculated from the reflectance values and the stratigraphic position of reflectance maxima and minima.

the sum of a constant and an exponential raised to the power of an exponent multiplied by the carbonate content yield nearly identical parameters at the different sites (Herbert *et al*. 1999). I use the value of reflectance at the 700 nm wavelength in this paper as a proxy for climatic variations, rather than carbonate content, because the reflectance data have a more Gaussian distribution than the carbonate transform. Data with Gaussian distributions are preferable for spectral analysis, and make a better model to compare with the precessional forcing which likely drove much of the variation in pelagic sedimentation in these drill sites.

A sample interval from DSDP Site 516F displays the modulated character of the reflectance data which will be discussed in more detail below (figure 2). One can, in addition to studying the reflectance values in the depth (time) domain, extract two types of modulation that contain valuable information. I employ a crude amplitude demodulation by measuring sequential peak–trough variations in the reflectance values of each *ca.* 20 ka long carbonate cycle (figure 2). This procedure removes variations in the mean reflectance (carbonate) values, and allows us to assess the variations in the amplitude of the sedimentary cycles as a function of stratigraphic depth or time. One can also look at the sequential variations in the stratigraphic thickness of carbonate cycles—an FM demodulation technique (Park & Herbert 1987). Provided that the orbital hypothesis is correct, these time-series (see figure 2) include variations due to both the inherent variability of the precessional period itself, and variations due to changes in depositional rate (Herbert 1994). These procedures are certainly more subjective than numerical demodulation techniques. However, I calculate moving window frequency spectra (*ca.* 300 ka time windows) to confirm objectively the identification of sedimentary cyclicity prior to the demodulations, and the procedure I employ has the advantage of being insensitive to coring gaps.

4. Evidence for groupings of carbonate cycles corresponding to 97, 123, 404 and 2425 ka modulations of precessional amplitude

Previous work has established that the mean period of repetition of carbonate cycles in Late Cretaceous (latest Santonian) through Early Palaeocene (chron C27n) time in the South Atlantic is very nearly 20 ka, in good agreement with the expected mean precessional period for this time (Herbert & D'Hondt 1990; Park *et al*. 1993). Lithological cycles in marine sediments of similar age attributed to precession have been documented in the Basque country of Spain (Ten Kate & Sprenger 1993) and in the Exmouth Plateau region of the Indian Ocean (Huang *et al*. 1992; Boyd *et al*. 1994). Our best hope for using the cycles to construct an integrated GPTS will come from recognizing modulation patterns of precessional cycles imprinted in sediments. Modulation gives character to cyclic waveforms that make it far easier to correlate cycles from one section to another than if the cycles were of constant amplitude. Correlation of cycles between study sections will be needed to construct a composite orbital chronology of the GPTS, and to test the completeness of an orbital reference model as new sections are acquired.

Eccentricity produces, in fact, a hierarchy of modulations centred around dominant periods of about 97, 123, 404, 2000 and 2800 ka (analysis of calculations of Laskar *et al*. (1993)). The 404 ka and longer modulations may play a particularly important role in time-scale construction because they are of a similar scale to other stratigraphic control points (e.g. similar to magnetic reversal frequency, extinction/speciation events in the fossil record, secular changes in the Sr isotope composition of the oceans, etc.). Hilgen (1991*a*, *b*) and colleagues have demonstrated how the high amplitude excursions of precession appear in lithological form as sapropel layers in the Late Miocene through Pleistocene of the eastern Mediterranean. The South Atlantic sequences of the Late Cretaceous and Early Palaeocene provide less extreme changes in lithology, but a similar grouping of packets of higher- and lower-amplitude carbonate cycles.

The short reversed-polarity chron C30r provides one instance in which we can directly correlate 97 ka modulation packets of Late Cretaceous carbonate cycles at least within the South Atlantic Basin. At typical pelagic deposition rates of 1–2 cm ka^{-1}, the chron (nominal duration of 125 ka: Cande & Kent 1995) should occupy

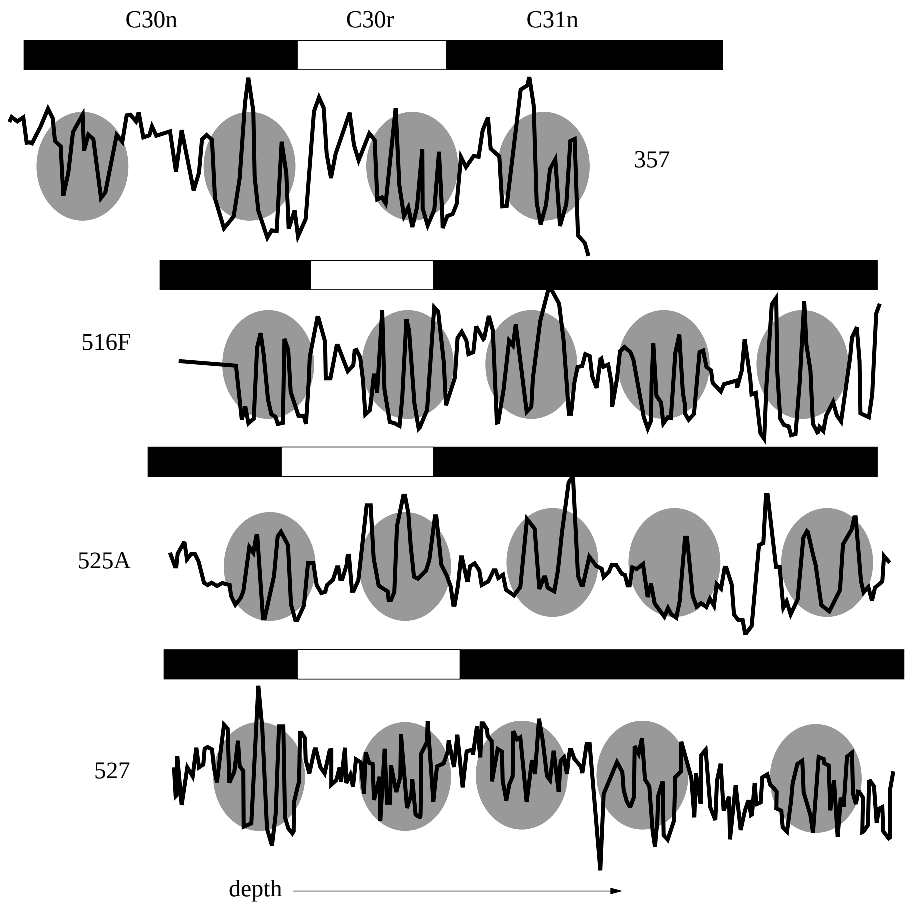

Figure 3. Correlation of *ca.* 100 ka carbonate modulation cycles through the magnetic polarity interval of chron C30r. The bars above each site refer to the measured polarity pattern (black = normal polarity) keyed to lithological variations. The nominal duration of the reversed-polarity zone (white bar) is 125 ka (Cande & Kent 1995). Note that the cycle pattern occupies a pattern relative to the polarity zone that is correlatable between sites.

between 1 and 2 m of section, or be contained entirely within the 9.5 m standard core interval of deep sea drilling. The South Atlantic study sites indeed provide four repetitions in which the chron is captured within a standard core, and hence is likely to have been preserved without major gaps. Figure 3 displays the pattern of carbonate cycles tied to magnetostratigraphy around the interval of Late Cretaceous time defined by chron C30r. Magnetic reversal boundaries have been determined at each site to an uncertainty of 5–40 cm, depending on the site, or 3–27 ka at typical sedimentation rates. One would expect to find six carbonate cycles of average period 20.4 ka each (Late Cretaceous precessional period interpolated from values in Berger *et al.* (1989)) between the polarity boundaries to correspond to the 125 ka duration estimated by Cande & Kent (1995), as indeed figure 3 demonstrates. My analysis actually indicates a number closer to five carbonate cycles, but this figure clearly overlaps with the GPTS when one considers the uncertainties in defining

PHILOSOPHICAL TRANSACTIONS OF THE ROYAL SOCIETY A MATHEMATICAL, PHYSICAL & ENGINEERING SCIENCES

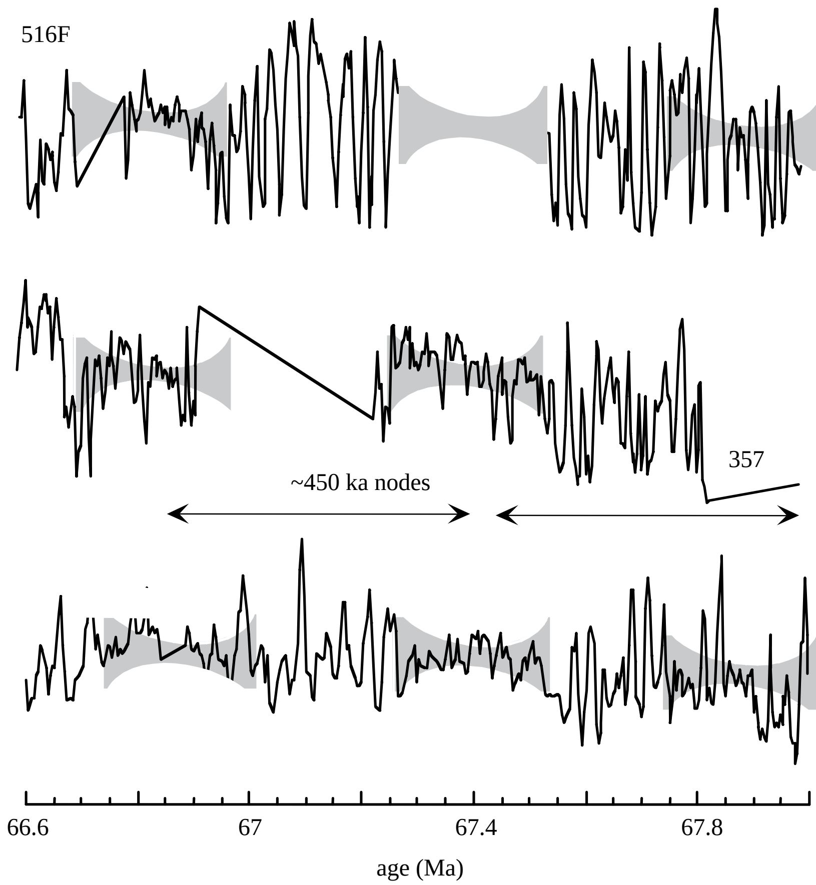

Figure 4. Example of *ca.* 404 ka cycles in the modulation of the amplitude of carbonate cycles correlated between the four South Atlantic study sites. The chronology for each site comes from the GPTS of Cande & Kent (1995). Note that a node of low variability at Site 516F has been lost by coring; compositing between drill sites generates a more continuous cyclochronology.

the precise positions of the polarity boundaries at each core site, in defining cycles precisely, and in determining the duration of short polarity intervals from sea-floor magnetic anomaly patterns. As importantly, it is clear that the peaks and nodes of cycle amplitude fall in a consistent position relative to the independent time framework provided by magnetostratigraphy. The base of chron C30r coincides with the first of three high-amplitude carbonate cycles evident at Sites 357, 516F, 525A and 527. A node of two low-amplitude cycles succeeds these, and the termination of the reversed-polarity interval occurs at the first cycle of the next packet of high amplitude cycles.

Although frequently interrupted by coring gaps, the *ca.* 404 ka modulation of precession also emerges as a pattern of nodes of 8–12 low-variability carbonate cycles that alternate with a similar number of high amplitude cycles (figure 4). Note that the estimated duration of the nodal pattern is somewhat longer than expected for the 404 ka eccentricity modulation of precession. This could be because I used a palaeomagnetically determined sedimentation rate that does not resolve accumula-

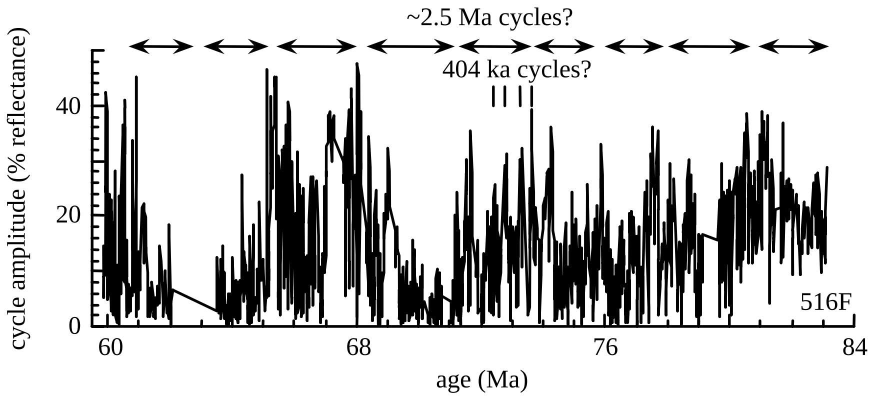

Figure 5. Amplitude modulations (see figure 2 for illustration of methods) of carbonate cycles at Site 516F. Note the alternation of packets of higher and lower amplitude at two scales that closely match the 404 and 2425 ka eccentricity modulations of precession.

tion rate changes adequately and therefore distorts the time-scale, because errors in the dating of the GPTS introduce absolute errors into the mean sedimentation rate estimate, or because of uncertainties in defining a cycle duration based on few repetitions. One can test the consistency of the presumed 404 ka modulation of carbonate bedding cycles by analysing longer amplitude demodulation series constructed by the method displayed in figure 2. Site 516F provides the longest series of carbonate cycles; an *ca.* 23 Ma record of amplitude modulation is presented in figure 5. The *ca.* 100 ka modulation evident in figures 2 and 3 disappears at this scale of presentation. Instead, packets of higher and lower amplitudes recur at sub- and supra-Ma scales. Coring gaps interfere with recognizing every sub-Ma packet. Nevertheless, I obtain 43 ± 3 such packets for the 18 Ma of Late Cretaceous time, for a nominal duration of 420 ka. Similar duration features persist into the more poorly recovered Palaeocene section at Site 516F (figure 5).

Very long wavelength organization of sedimentary variations gives an average period of 2.5 Ma (figure 5). I subjectively recognize one such cycle peak in the interval of the missing section between about 62.5 and 64 Ma, to obtain a total of eight full cycles between 61 and 81 Ma. These cycles vary in apparent period from 1.7 to 3.5 Ma. This pattern is not dissimilar to the *ca.* 2.4 Ma modulation of precession derived over the last 10 Ma, which produces nodal patterns that alternately jump between 2020 and 2828 ka repetitions (Laskar *et al*. 1993).

5. Implications of orbital chronology for the latest Cretaceous and Early Palaeocene time-scale

Obtaining an accurate chronology for the interval of time spanning the K–T boundary has important implications for measuring the pace of events across this major event in the Earth's history. Herbert & D'Hondt (1990) and Herbert *et al*. (1995) presented results of precessional chronometry derived from compositing cyclic sections between South Atlantic drill sites within the magnetostratigraphic framework of chron C29r. The results (18.5 ± 1 cycle for the Cretaceous interval of the reversed-polarity chron, and 13 ± 1 cycles for the earliest Palaeocene interval) seem consistent

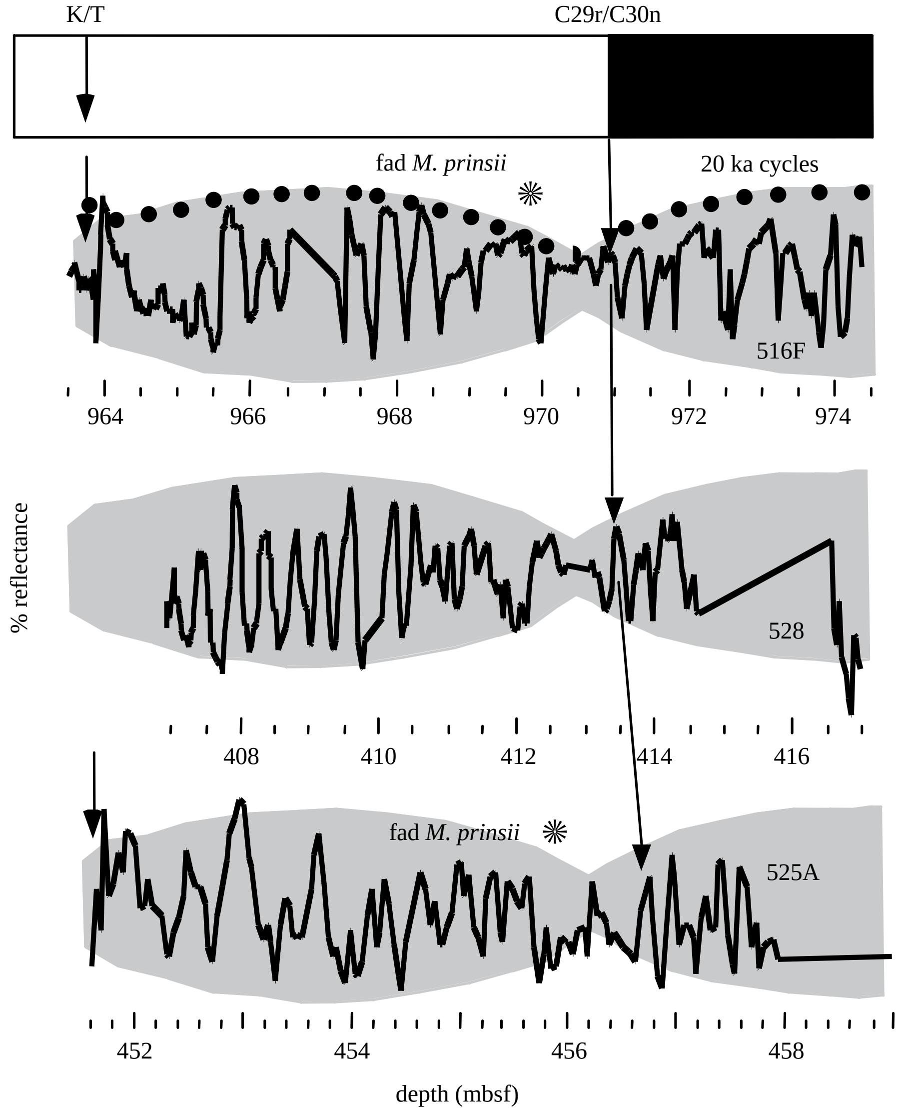

Figure 6. Precessional chronology of latest Maastrichtian sediments in the South Atlantic, relative to high-resolution magnetostratigraphy, and the terminal Cretaceous nannofossil datum, the last appearance of *M. prinsii* (Henriksson 1993). Note that the transition from polarity chron C30n to C29r occurs in a node of low amplitude carbonate cycles determined by the 404 ka modulation of precession. Note also the *ca.* 97 ka modulations of carbonate cycles within chron C29r that permit compositing between sections.

with cycle patterns at the Zumaya Section documented by Ten Kate & Sprenger (1993). A similar subdivision of Cretaceous and earliest Palaeocene time within chron C29r was obtained by Shackleton (1984), who extrapolated sedimentation rates above and below the reversed-polarity zone to estimate the latest Cretaceous and earliest Tertiary sedimentation rates in Walvis Ridge sediments. Figure 6 shows the composite section of latest Maastrichtian cyclic sedimentation in the South Atlantic. Note

PHILOSOPHICAL TRANSACTIONS OF THE ROYAL SOCIETY A MATHEMATICAL, PHYSICAL & ENGINEERING SCIENCES

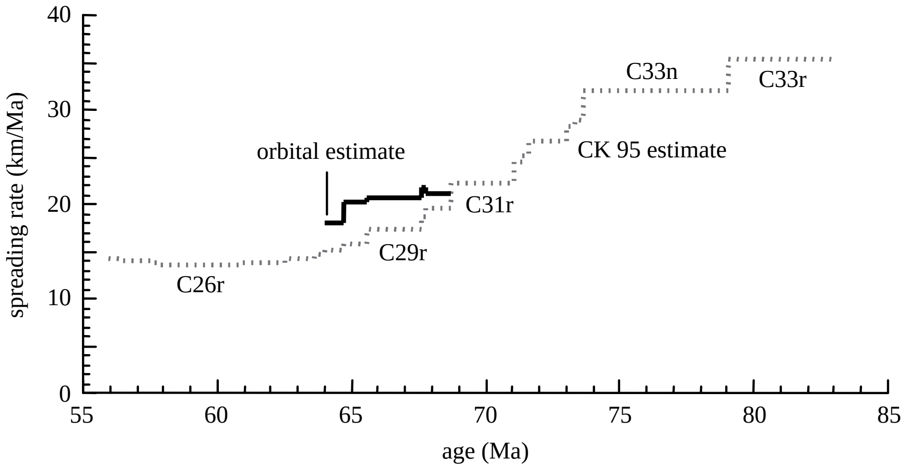

Figure 7. South Atlantic spreading rates calculated by Cande & Kent (1995) from distances of magnetic anomalies from the Mid-Atlantic Ridge using their spreading rate model, compared with estimates obtained by combining magnetic anomaly distances with durations estimated by counting precessional carbonate cycles.

that the chron C29r–C30n boundary occurs at each site in a node of low variability dictated by the *ca.* 404 ka cycle of modulation. The field study of Ten Kate & Sprenger (1993) extends the cyclostratigraphy upward through chron C29n, although one should note that this study relied on correlating bedding levels documented at the Zumaya Outcrop to another outcrop section with magnetostratigraphy. Herbert *et al.* (1995) deduced 32 ± 2 cycles in the C29n sequence at Zumaya, for a duration of 653 ka. As indicated in figures 3 and 4, the South Atlantic sequence can be composited through to the chron C31n–C31r boundary with good confidence. I obtain durations for chron C30n of 1.7 Ma, for chron C30r of 0.105 Ma, and for chron C31n of 0.925 Ma.

What consequences do these revisions to the GPTS of Cande & Kent (1992, 1995) have? Orbital chronometry shortens the time span of chrons C29n and C29r, which contain the K–T boundary and the Early Palaeocene faunal and floral recoveries, by *ca.* 20%. Polarity durations determined by cyclochronology are *ca.* 15% shorter for chron C30n and 5% shorter from chron C31n. These revised durations, if confirmed by study at other sections, have implications for the spreading rate behaviour of the South Atlantic, which provides the reference section for the Cande & Kent (1992, 1995) time-scale. The Cande & Kent time-scale fits a smooth spline curve through a small number of tie-points to link the sea-floor anomaly pattern to time. Figure 7 converts the South Atlantic anomaly block pattern to apparent spreading rates, using ages according to the Cande & Kent (1992, 1995) studies. The Cande & Kent time-scale infers a significant slowing of spreading rate in the South Atlantic from chron C33r (Campanian) to chron C29r (*ca.* 65 Ma). The coincidence of the decline in spreading rate with chron C29r comes from the use of a K–T boundary date (65.1 Ma) as a radiometric tie-point in a sparse set of numerical ages available. Our orbital chronology suggests that the reduction in spreading rate from Late Cretaceous through Early Palaeocene time was significantly gentler than the model of Cande & Kent would imply. Provided that one accepts the numerical tie-points used by

Cande & Kent (1995), the integral of an orbital chronology ought to converge with the integral of the Cande & Kent (1995) polarity durations. The somewhat shorter durations estimated for the Late Cretaceous and Early Palaeocene magnetochrons by cyclostratigraphy must, if correct, be compensated by more time elsewhere in the GPTS. An implication of the orbital model shown in figure 7 is, therefore, that the Cande & Kent (1995) GPTS must have underestimated the durations of chrons C32–C33, and hence overestimated the South Atlantic spreading rate during this time. One could also conclude that sea-floor spreading rates decelerated less from the Cretaceous long normal polarity interval into the Late Cretaceous mixed polarity interval than currently envisioned.

6. Conclusions

While precession provides the fundamental pacing of carbonate–marl cycles in pelagic sediments of the South Atlantic over a time span of at least 30 Ma, the lithological contrast between adjacent strata comes from the amplitude modulation periods of precession. Most of the variation in amplitude, even at relatively long wavelengths (e.g. from 400 to 3000 ka) is organized according to periods very similar to the dominant 97, 404 and 2425 ka modes of eccentricity modulation calculated from astronomical solutions valid for the past few tens of millions of years (Berger *et al*. 1992; Laskar *et al*. 1993). Changes in sedimentation due to long-term trends in sea level, tectonically controlled variations in geochemical cycling, and other non-orbital influences apparently do not overwhelm the astronomical influence on sedimentation. Prospects appear to be excellent that a complete record of the Late Cretaceous–Palaeocene modulating frequencies of precession can be extracted from sediments keyed to magnetic reversal stratigraphy, provided that several more sections can be drilled to fill in gaps left by previous ocean drilling. The modulated patterns will be useful for correlating between study locations and for refining the durations of magnetic polarity intervals in the GPTS. There remains the significant challenge of stitching the patterns documented here into an orbital chronology continuous up to the present.

References

Berger, A., Loutre, M. F. & Dehant, V. 1989 The influence of the changing lunar orbit on the astronomical frequencies of the pre-Quaternary insolation patterns. *Paleoceanography* **4**, 555–564.

Berger, A., Loutre, M. F. & Laskar, J. 1992 Stability of the astronomical frequencies over the Earth's history for paleoclimate studies. *Science* **255**, 560–566.

Berggren, W. A., Kent, D. V., Swisher II, C. C. & Aubry, M.-P. 1995 A revised Cenozoic geochronology and chronostratigraphy. In *Geochronology time scales and stratigraphic correlation* (ed. W. A. Berggren & D. V. Kent). Society of Economic Paleontologists and Mineralogists Spec. Publ., no. 54, pp. 129–212. Tulsa, OK: Society for Sedimentary Geology.

Boersma, A. 1984 Cretaceous–Tertiary planktonic foraminiferas from the south-eastern Atlantic, Walvis Ridge area, Deep Sea Drilling Project Leg 74. *Initial Rep. DSDP* **74**, 501–523.

Boyd, R., Huang, Z. & O'Connell, S. 1994 Milankovitch cyclicity in Late Cretaceous sediments from Exmouth Plateau off northwest Australia. In *Orbital forcing and cyclic sequences* (ed. P. L. de Boer & D. G. Smith). *Spec. Publ. Int. Ass. Sed.* **19**, 145–166.

Cande, S. C. & Kent, D. V. 1992 A new geomagnetic polarity time scale for the Late Cretaceous and Cenozoic. *J. Geophys. Res.* **97**, 13 917–13 951.

Cande, S. C. & Kent, D. V. 1995 A revised calibration of the geomagnetic polarity time scale for the Late Cretaceous and Cenozoic. *J. Geophys. Res.* **100**, 6093–6095.

Chave, A. D. 1984 Lower Paleocene–Upper Cretaceous magnetic stratigraphy from Sites 525, 527, 528, and 529. *Initial Rep. DSDP* (ed. T. C. Moore Jr and 14 others), vol. 74, pp. 525–531.

Curry, W. B., Shackleton, N. J. & Richter, C. (eds) 1995 *Proc. ODP Initial Rep.* 154.

D'Hondt, S., King, J. & Gibson, C. 1996 Oscillatory marine response to the Cretaceous–Tertiary impact. *Geology* **24**, 611–614.

Gee, J. & Herbert, T. D. 1999 Magnetic polarity stratigraphy of cyclic Late Cretaceous to Palaeocene sediments from the South Atlantic. (In preparation.)

Hamilton, N. & Suzyumov, A. E. 1983 Late Cretaceous magnetostratigraphy of Site 516, Rio Grande Rise, southwestern Atlantic Ocean, Deep Sea Drilling Project, Leg 72. *Initial Rep. DSDP* **72**, 723–730.

Henriksson, A. S. 1993 Biochronology of the terminal Cretaceous calcareous nannofossil zone of *Micula prinsii*. *Cret. Res.* **14**, 59–68.

Herbert, T. D. 1994 Reading orbital signals distorted by sedimentation: models and examples. In *Orbital forcing and cyclic sequences* (ed. P. L. deBoer & D. G. Smith). *Spec. Publ. Int. Ass. Sed.* **19**, 483–507.

Herbert, T. D. & D'Hondt, S. L. 1990 Precessional climate cyclicity in Late Cretaceous–Early Tertiary marine sediments: a high resolution chronometer of Cretaceous–Tertiary boundary events. *Earth Planet. Sci. Lett.* **99**, 263–275.

Herbert, T. D., Erba, E., Premoli Silva, I. & Fischer, A. G. 1995 Orbital chronology of Cretaceous–Paleocene marine sediments. In *Geochronology, time scales and global stratigraphic correlation* (ed. W. A. Beggren, D. V. Kent, M. P. Aubry & J. Hardenbol). Society of Economic Paleontologists and Mineralogists Spec. Publ., no. 54, pp. 81–93. Tulsa, OK: Society for Sedimentary Geology.

Herbert, T. D., Gee, J. & DiDonna, S. 1999 Precessional climatic cycles in the Late Cretaceous South Atlantic: long-term consequences of high-frequency variations. In *Late Cretaceous climates* (ed. E. Barrera & C. Johnson). Society of Economic Paleontologists and Mineralogists Spec. vol. 322. Tulsa, OK: Society for Sedimentary Geology.

Hilgen, F. J. 1991*a* Astronomical calibration of Gauss to Matuyama sapropels in the Mediterranean and implication for the geomagnetic polarity time scale. *Earth Planet. Sci. Lett.* **104**, 226–244.

Hilgen, F. J. 1991*b* Extension of the astronomically calibrated (polarity) time scale to the Miocene/Pliocene boundary. *Earth Planet. Sci. Lett.* **107**, 349–368.

Huang, Z., Boyd, R. & O'Connell, S. 1992 Upper Cretaceous cyclic sediments from ODP Hole 122-762C–Exmouth Plateau, N.W. Australia. In *Proc. ODP Sci. Results* (ed. U. von Rad and 28 others), vol. 122, pp. 259–277.

Laskar, J. 1990 The chaotic motion of the Solar System: a numerical estimate of the size of the chaotic zones. *Icarus* **88**, 266–291.

Laskar, J., Joulet, F. & Boudin, F. 1993 Orbital, precessional, and insolation quantities for the Earth from −20 Myr to +10 Myr. *Astron. Astrophys.* **270**, 522–533.

Manivit, H. & Feinberg, H. 1984 Correlation of magnetostratigraphic and nannofossil biostratigraphy in upper Cretaceous and lower Paleocene sediments of the Walvis Ridge area. In *Initial Rep. DSDP* (ed. T. C. Moore Jr and 14 others), vol. 74, pp. 469–474.

Moore Jr, T. C., Rabinowitz, P. D., Borella, P. E., Shackleton, N. J. & Boersma, A. 1984 History of Walvis Ridge. *Initial Rep. DSDP* (ed. T. C. Moore Jr and 14 others), vol. 74, pp. 873–894.

Park, J. & Herbert, T. D. 1987 Hunting for paleoclimatic periodicities in a sedimentary series with uncertain time scale. *J. Geophys. Res.* **92**, 14 027–14 040.

Park, J., D'Hondt, S. L., King, J. W. & Gibson, C. 1993 Late Cretaceous precessional cycles in double time: a warm Earth Milankovitch response. *Science* **261**, 1431–1434.

Perch-Nielsen, K. 1977 Aptian to Pleistocene calcareous nannofossils from the western south Atlantic, DSDP Leg 39. *Initial Rep. DSDP* (ed. P. R. Supko and 11 others), vol. 39, pp. 699–824.

Premoli Silva, I. & Boersma, A. 1977 Cretaceous planktonic foraminifers—DSDP Leg 39 (South Atlantic). *Initial Rep. DSDP* **39**, 615–641.

Ruddiman, W. F., Cameron, D. & Clement, B. M. 1987 Sediment disturbance and correlation of offset holes drilled with the hydraulic piston corer: Leg 94. *Initial Rep. DSDP* **94**, 615–634.

Shackleton, N. J. 1984 Accumulation rates of Leg 74 sediments. *Initial Rep. DSDP* **74**, 645–662.

Shackleton, N. J., Berger, A. & Peltier, W. R. 1990 An alternative astronomical calibration of the lower Pleistocene time scale based on ODP Site 677. *Trans. R. Soc. Edinb.* **81**, 251–261.

Ten Kate, W. G. H. & Sprenger, A. 1993 Orbital cyclicities above and below the Cretaceous/Paleogene boundary at Zumaya (N. Spain), Agost and Relleu (SE Spain). *Sed. Geol.* **87**, 69–101.

Wilson, D. S. 1993 Confirmation of the astronomical calibration of the magnetic polarity time scale from sea-floor spreading rates. *Nature* **364**, 788–790.